Hydrodynamic approach to electron-hole droplet nucleation and stability

Richard N. Silver
Theoretical Division, Los Alamos Scientific Laboratory, Los Alamos, New Mexico 87545
(Received 4 October 1977)

A hydrodynamic model for the nonequilibrium thermodynamics of electron-hole droplets in semiconductors is presented. It predicts droplet properties at densities and temperatures where the assumptions of nucleation kinetics fail. It is an extension to finite lifetimes of the Cahn-Hilliard theories of critical droplets and spinodal decomposition. As in finite-lifetime nucleation kinetics both critical and stable droplets are found to exist above a minimum supersaturation which must become large at low temperatures. However, stable droplets differ both quantitatively and qualitatively from the capillarity approximation commonly assumed in nucleation kinetics. For example, they may be characterized by a velocity profile which peaks in the surface region. Among other novel predictions are that: (i) a maximum supersaturation before phase separation is given by the spinodal line; (ii) stable droplets continue to exist at temperatures approaching T_c but their properties are strongly affected by impurity and phonon scattering; and (iii) at very low temperatures critical droplets are too small for hysteresis, but stable droplet properties are calculated. Quantitative predictions are made by the principle of corresponding states.

I. INTRODUCTION

In many respects electron-hole condensation in semiconductors has been shown to be analogous to other liquid-gas transitions.[1] However, among the several important differences is the one that in semiconductors the condensing particles have finite lifetimes. The nonequilibrium character of electron-hole condensation is manifest in experiments on nucleation, droplet-size distributions, optical hysteresis, and especially in strong departures from ordinary liquid-gas behavior at low temperatures.[2-5] At temperatures well below the critical temperature ($T<4$ °K in Ge) and at excitations near the thresholds for droplet formation and decay, these experiments[2-5] have been successfully described by the generalization of nucleation kinetics to finite lifetimes.[6,7]

For ordinary liquid-gas transitions, the controlling variable in nucleation is the Gibbs free energy as a function of droplet size. For gas densities $\bar{n}$ greater than the coexistence curve n_g, there is a net lowering in free energy due to formation of the liquid phase. However, there is also a net gain in free energy due to formation of the interface between gas and liquid. The first term is proportional to the droplet volume, while the second is proportional to surface area. A critical radius is defined by the size where bulk and surface contributions to the change in free energy with size are balanced. Larger droplets find it energetically favorable to continue growth, while smaller droplets find it energetically favorable to evaporate. Dynamically for $\bar{n}>n_g$, droplets larger than critical collect gas particles faster than they evaporate them. The interface free energy has the effect of increasing the evaporation rate for small droplets. The nucleation rate is controlled by the formation of critical droplets by statistical fluctuations. This rate is proportional to minus the exponential of the Gibbs energy of a critical droplet. This energy and the corresponding critical radius decrease with increasing supersaturation ($S=\bar{n}/n_g - 1$) and with decreasing surface tension (which determines the interface free energy). Droplets once formed continue growing for any $S>0$ provided their size is greater than the critical radius.

For electron-hole liquids the new feature is the finite particle lifetimes due to recombination. Dynamically, the lifetimes provide a new mechanism for droplets to lose particles at a rate proportional to the droplet volume. The evaporation and collection rates are proportional to droplet surface area. Thus, one expects another characteristic droplet radius to be determined by the size where the net collection of particles for $\bar{n}>n_g$ is balanced by the net loss of particles due to recombination. Larger droplets will tend to lose particles reducing toward the characteristic radius. Smaller droplets will tend to gain particles growing toward the characteristic radius. Therefore, this radius is termed the "stable" droplet radius. Since the net difference between collection and evaporation rates increases from zero as the supersaturation increases from zero, the stable droplet size should increase with supersaturation. Note that the concept of a stable droplet does not depend on surface tension.

Consider then what happens when both the surface tension is nonzero and the lifetime is finite. For high supersaturations, the stable radius will be large while the critical radius will be small. As the supersaturation is reduced, the two characteristic radii will approach one another until, at what is termed a minimum supersaturation $S_{\min}$,

critical and stable radii are equal. At supersaturations $S<S_{min}$ there are no droplet sizes where the particle collection rate exceeds the combined effect of a lifetime loss proportional to droplet volume and a surface evaporation term enhanced by the effect of interface free energy. Note also that the surface rates of evaporation and collection decrease rapidly with decreasing temperature, while the lifetime loss is temperature independent. Thus, S_{min} must become large at low temperature.

This description follows the language of nucleation kinetics. However, an alternative description may be provided by hydrodynamics. In the rest of the Introduction, the two approaches will be compared with regard to the assumption involved, the domain of applicability, and the nature of their predictions.

The detailed assumptions of nucleation kinetics are that[8]: (i) particles undergo free molecular flow apart from collisions; (ii) kinetic equations for the concentrations of particle cluster sizes are applicable; (iii) the rates are determined by gas kinetic collision cross sections and detailed balance; (iv) monomers are the dominant cluster size; and (v) the Gibbs energy of a large cluster is given by the "capillarity approximation" in which there is a volume term proportional to the difference in chemical potentials of gas and liquid and a surface term proportional to the bulk surface tension.[9,10] Clearly, assumptions (i)–(iv) require an almost ideal gas phase and, therefore, that the kinetic energy is much larger than the potential energy of particles in the gas phase. This is not true at high supersaturations, near the critical point, and near the spinodal line separating metastable from unstable regions of the phase diagram. The capillarity approximation, assumption (v), can be established from a microscopic basis for the critical droplets which control nucleation,[11] but it has not been established for the stable droplets which are unique to electron-hole condensation because of the finite lifetimes.

In order to address these difficulties, in this paper an alternative hydrodynamic approach to the nonequilibrium thermodynamics of electrons and holes is presented. The hydrodynamic model is a continuum approximation to the behavior of a condensing fluid. It consists of combining the density functional formalism, which has been applied to surface properties,[12] with the hydrodynamic equations of change. The equation of continuity is modified to include particle creation and recombination. The equation of motion is modified to include frictional forces due to scattering from phonons and impurities. The equation of state is nonmonotonic below a critical temperature corresponding to a liquid-gas transition. This formulation has a precursor in the Cahn-Hilliard theory of critical droplets and spinodal decomposition.[11,13] In the infinite lifetime limit, it can be used to derive the capillarity approximation for critical droplets. It also describes the alternative phase separation mechanism of the exponential growth of density fluctuations (spinodal decomposition) at extremely high supersaturations where the ideal gas assumption is invalid.[13]

The unique feature of this paper is to present the predictions of the hydrodynamic model for the finite lifetimes appropriate to electrons and holes in semiconductors. Despite the qualitatively different character of hydrodynamics and nucleation kinetics, as shall be shown, the two theories share many predictions for droplet properties in the ideal gas phase region. Both predict the existence of stable and critical droplets above a minimum supersaturation, that the minimum supersaturation increases with decreasing temperature, and that strong departures from ordinary liquid-gas behavior must occur at low temperatures. Further, both theories may be scaled in terms of critical-point parameters to depend only on one dimensionless variable $\xi \simeq m\sigma^2/\tau^2(kT_c)^3 n_c^3$, where σ is surface tension at 0 °K, τ is lifetime, m is mass, T_c is critical temperature, and n_c is critical density.

However, the hydrodynamic model may be applied in regions of density and temperature where the ideal-gas assumption of the nucleation kinetics model breaks down. These include (a) temperatures below that where the minimal supersaturation becomes comparable to one ($T<T_0$), (b) near the critical temperature, (c) near the spinodal line separating metastable from unstable regions of the phase diagram, and (d) inside the spinodal region. Further, even in the ideal-gas region hydrodynamics makes new predictions for droplet properties such as size, density, chemical potential, density profile, etc., which differ from the results and assumptions of nucleation kinetics. In particular, the properties of stable droplets differ substantially from the capillarity approximation. These predictions may be tested by the standard experiments in luminescence, light scattering, junction noise, etc.

Time-dependent phenomena are another area where hydrodynamics differs from nucleation kinetics. Because it is a continuum approximation, hydrodynamics does not have the statistical fluctuations responsible for nucleation and decay. This may be remedied by adding suitable Langevin forces to the equations and deriving a Fokker-Planck equation for the distribution of hydrodynamic variables density and velocity.[14] This subject will be addressed in a later paper.

The organization of this paper is as follows.

Section II is concerned with formulating the hydrodynamic model. Section II A presents a brief review of relevant concepts and results in the theory of phase transitions and critical droplets. Section II B is a presentation of the equations of the model. Section II C discusses the applicability of the hydrodynamic model. Section II D shows how the principle of corresponding states can be used to make quantitative predictions. Section III contains a treatment of the zero surface tension limit of the droplet solutions of the hydrodynamic equations. In Sec. IV droplet solutions of the complete equations are studied. Section IV A discusses numerical solutions. Section IV B introduces a very useful approximation. Section IV C contains a derivation of droplet properties such as minimum supersaturation and minimum radius in this approximation. Section IV D studies droplet behavior at densities near the spinodal line. Section IV E discusses droplet behavior at low temperatures. Section V contains a summary and discussion. In Appendix A properties of the model equation of state used in the numerical work are presented. Appendix B contains a derivation of a sum rule used repeatedly in Sec. IV. Appendix C discusses the effect of a nonzero friction coefficient. Appendix D presents a "cell model" for predicting the behavior at high excitation when the droplets are interacting with each other. Appendix E contains a summary of some of the principal results of nucleation kinetics in a form suitable for comparison with the hydrodynamic model.

A preliminary account of this work has been published elsewhere.[15]

II. FORMULATION OF THE HYDRODYNAMIC MODEL

A. Review of concepts in the theory of surface tension and phase transitions

The equation of state of a system of particles may be specified in terms of the free energy per unit volume f, pressure p, or chemical potential μ as functions of the density n and temperature T. These quantities are related by $p=n\mu-f$ and $\mu=df/dn$. Above the critical temperature p and μ are monotonically increasing functions of n. Below the critical temperature there is a mechanically "unstable" region of the n,T plane where $d\mu/dn$ is negative. The "spinodal line" n_s defined by $(d\mu/dn)|_{n_s}=0$ separates metastable from unstable regions. A second line termed the "coexistence curve" defined by $p(n_l)=p(n_g)$ and $\mu(n_l)=\mu(n_g)$ separates metastable from stable regions. A metastable state may be defined as a system which could lower its free energy by separating into high- and low-density fluids but there is a free-energy barrier to its doing so. These various regions are

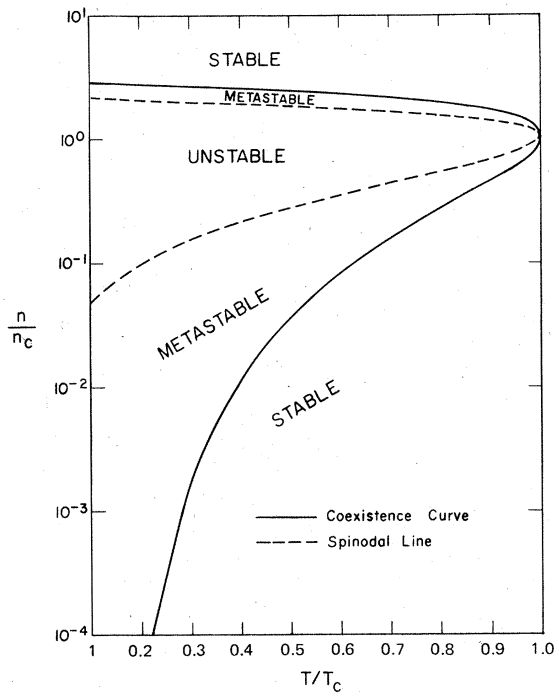

FIG. 1. Schematic phase diagram for electron-hole fluids calculated using the model equation of state in Appendix A. Solid line is the coexistence curve. Dashed line is the spinodal curve. The development of equations of state for electron-hole fluids in semiconductors is required for realistic determination of these curves.

illustrated in Fig. 1 for the model equation of state discussed in Appendix A.

For an inhomogeneous system of ordinary particles, the density gradient approximation to its free energy is given by[10,11,13]

$$F(n)=\int d^3r\,[\tfrac{1}{2}K(\nabla n)^2+f(n)]. \tag{1}$$

Consider first a plane interface between liquid and gas phases. Variation of $F(n)$ with respect to $n(x)$ gives

$$K\frac{d^2n}{dx^2}=\mu(n)-\mu(n_g). \tag{2}$$

This may be integrated to

$$\frac{dn}{dx}=\left(\frac{2}{K}\{p(n_g)-p(n)+n[\mu(n)-\mu(n_g)]\}\right)^{1/2}, \tag{3}$$

as the equation describing the surface density profile. For A equal to surface area the free energy (1) is

$$F(n(x))-F(n_g)=A\int K\left(\frac{dn}{dx}\right)^2dx + A\int(n-n_g)\mu(n_g)\,dx. \tag{4}$$

The surface free energy is therefore

$$\sigma = \int_{-\infty}^{\infty} K\left(\frac{dn}{dx}\right)^2 dx$$

$$= \int_{n_g}^{n_l} (2K)^{1/2}\{p(n_g) - p(n) + n[\mu(n) - \mu(n_g)]\}^{1/2}\, dn. \tag{5}$$

The width of the interface profile W is on the order of

$$W = (n_l - n_g)^2 K/\sigma. \tag{6}$$

Consider next extrema of $F(n)$ for spherically symmetric droplets. The density profile must satisfy

$$K\frac{d^2n}{dr^2} + \frac{2K}{r}\frac{dn}{dr} = \mu(n) - \mu(\bar{n}), \tag{7}$$

where $\bar{n}$ is the average density in the gas phase.

A numerical study of Eq. (7) confirms that the following approximate treatment is valid provided the droplet surface radius r_s is greater than the plane interface width W [Eq. (6)]. Then dn/dr is large only in the surface region and negligible elsewhere. To use this observation, multiply (7) by dn/dr and integrate to obtain

$$\frac{K}{2}\left(\frac{dn}{dr}\right)^2\Bigg|_r + \int_{\infty}^{r} \frac{2K}{r}\left(\frac{dn}{dr}\right)^2$$

$$= f(n(r)) - f(\bar{n}) - (n - \bar{n})\mu(\bar{n}). \tag{8}$$

When $r = 0$ and $r_s > W$, one has by assumption $\mu[n_0] = \mu(\bar{n})$ for $n_0 = n(0)$. Equation (8) then reduces to

$$p[n_0] - p(\bar{n}) = \int_0^{\infty} \frac{2K}{r}\left(\frac{dn}{dr}\right)^2 \cong \frac{2\sigma}{r_s}. \tag{9}$$

The droplet size is infinite at $\bar{n} = n_g$ and decreases with increasing supersaturation. The free energy may be calculated from (1) by substituting (8) into (1) and noting that

$$\int_{\infty}^{r} \frac{2K}{r}\left(\frac{dn}{dr}\right)^2 dr \simeq -\frac{2\sigma}{r_s}\Theta(r_s - r).$$

Then $F(n)$ is given by

$$F(n) \cong \tfrac{4}{3}\pi r_s^2\sigma + \tfrac{4}{3}\pi r_s^3(n_0 - \bar{n})\mu(\bar{n}), \tag{10}$$

and the Gibbs energy $G(n)$, defined by $F(n) - \mu(\bar{n}) \times \int d^3r\,[n(r) - \bar{n}]$, is equal to a positive quantity $\frac{4}{3}\pi r_s^2\sigma$. Equations (9) and (10) can be reduced to that of the standard capillarity approximation in the limit that $\bar{n} \ll n_l$ and small $\bar{n} - n_g$. Then one may show $p(n_0) - p(\bar{n}) \simeq n_l[\mu(\bar{n}) - \mu(n_g)]$. This gives

$$F(n) \cong 4\pi r_s^2\sigma + \tfrac{4}{3}\pi r_s^3 n_l \mu(n_g) \tag{11}$$

and

$$r_s \simeq 2\sigma/n_l[\mu(\bar{n}) - \mu(n_g)], \tag{12}$$

which are identical to the capillarity approximation results for critical droplets.

For $\bar{n}$ large enough for $r_s \lesssim W$ the above approximations cannot be justified and numerical solution of Eq. (7) must be obtained. The binary mixture analog of this equation has been studied by Cahn and Hilliard.[11,12] Numerical solutions which we have carried out confirm that the principal conclusions of Cahn and Hilliard remain valid in the liquid-gas case. For increasing supersaturation $\mu(n_0)$ falls increasingly below $\mu(\bar{n})$. The surface density profile becomes more extended and poorly defined. As $\bar{n}$ approaches the spinodal line, n_0 approaches the lower boundary of the spinodal n_s and the amount of matter contained in the critical droplet approaches zero. Numerical solutions show that $\int dr\,(dn/dr)^2$ starts at the plane interface value for large r_s but falls toward zero as r_s decreases.

B. Equations of the hydrodynamic model

Consider then a system of condensing particles of mass m and lifetime τ. The hydrodynamic variables are the density $n(\vec{r},t)$ and velocity $\vec{u}(\vec{r},t)$. For an inhomogeneous flowing fluid the free-energy functional is postulated to be[11,14]

$$F(n,\vec{u}) = \int d^3r\left(\frac{mn\vec{u}^2}{2} + \frac{K}{2}(\vec{\nabla}n)^2 + f(n)\right). \tag{13}$$

The first term is the kinetic energy contribution and the other terms are as discussed in Sec. II A. The equation of motion is the Euler equation

$$m\frac{\partial\vec{u}}{\partial t} = -m\vec{u}\cdot\vec{\nabla}(\vec{u}) - \vec{\nabla}[-K\nabla^2 n + \mu(n)] - m\beta\vec{u}. \tag{14}$$

Here a simple friction term $-m\beta\vec{u}$ has been added to the usual hydrodynamic equation to simulate scattering from impurities and phonons. Possible dissipative terms due to other damping mechanisms such as viscosity might also be added, but these will not be considered in this paper. The equation of continuity is taken to be

$$\frac{\partial n}{\partial t} = -\vec{\nabla}\cdot(n\vec{u}) - \frac{n}{\tau} + \frac{\bar{n}}{\tau}, \tag{15}$$

where the second term is due to recombination and the third term is due to excitation processes which maintain an average density $\bar{n}$. The dependence of τ on density has been ignored. It is assumed that photon transport is unimportant, which restricts this model to fluids in indirect-gap semiconductors

or in small samples of direct-gap material. Usually a third hydrodynamic equation is added to describe energy conservation. However, in high-purity semiconductors the phonon mean free path and consequent thermal conductivity are quite large at low temperatures. Further, no evidence for thermal disequilibrium between droplets and exciton gas has been observed in recombination spectra. This justifies an assumption of isothermal flow except for extremely high-intensity short-pulse excitation.

These equations potentially constitute a basis for the description of many diverse phenomena. In this paper attention is restricted primarily to stationary spherically symmetric droplet solutions. Then (14) and (15) become

$$u = -\frac{1}{4\pi r^2 n}\int_0^r \frac{4\pi r'^2(n-\bar{n})}{\tau}\,dr' , \tag{16}$$

and

$$\frac{Kd^2n}{dr^2}+\frac{2K}{r}\frac{dn}{dr}=\frac{mu^2}{2}+\mu(n)-\mu(\bar{n})-\int_r^\infty m\beta u\,dr , \tag{17}$$

where boundary conditions appropriate for an isolated fluctuation are chosen, i.e., $n \to \bar{n}$ and $u \to 0$ as $r \to \infty$. The average density $\bar{n}$ must be in the low-density metastable region for an isolated fluctuation. In Appendix D the case of nonisolated fluctuations and $\bar{n}$ in the unstable region is considered.

C. Applicability of the qualitative predictions of the hydrodynamic equations for droplet properties

The hydrodynamic model is clearly an extension to finite lifetimes of the density-functional formalism which can be used to derive the well-established capillarity approximation for critical droplets. The equations are certainly valid when the ratio of the mean free path to the distance scale of fluctuations in the hydrodynamic variables is small. They can also remain valid for large mean free paths in the sense that they reduce to conservation, or Euler, equations for the density, momentum, and energy moments of the Boltzmann equation.[16]

For droplets the mean free path varies between very short for the high-density liquid at droplet center to a larger value for the lower-density gas phase far from the droplet. If the mean free path is important, it will show up as a nonlocal relation between forces and gradients or, equivalently, as a limitation on the distance scale of fluctuations produced by transport coefficients. Therefore, the droplet radius must be large compared to the mean free path when transport coefficients are important.[17] For low-density excitons in germanium at helium temperatures, the mean free path due to phonon scattering is estimated to be between $\frac{1}{10}$ and $1\,\mu$m. The important droplet radii lie between 15 and $\frac{1}{100}$ μm which is the Bohr radius of an exciton.[2] Thus, hydrodynamics becomes a poorer approximation with decreasing droplet size.

However, there are several reasons why one may expect the hydrodynamic description to remain valid until rather small droplet sizes. First, it is shown in Appendix C that at low gas densities the transport coefficients are unimportant to the results. Second, as shall be shown, the density fluctuations in the gas phase are only on the order of $\sqrt{e}$. Third, in this limit the results are qualitatively similar to and only quantitatively different from the predictions of nucleation kinetics which is a free-molecular-flow approach.

Given the approximate validity of a hydrodynamic description, there is still the question of whether time-independent droplet solutions are the appropriate subject of study. In the limit of very small viscosity (large Reynolds number), most stationary solutions of Navier-Stokes equations are unstable. The extreme example of this is turbulence. (The viscosity is still important in producing dissipation at high momenta.) Time-dependent solutions may very well be important at low temperatures ($T \ll T_0$) where the stationary-droplet solutions cannot be found either in the hydrodynamic model or in nucleation kinetics, as shall be discussed. Limitations on quantitative predictions are discussed in Sec. II D.

D. Quantitative predictions, scaling, and the principle of corresponding states

The principle of corresponding states is applicable for a wide variety of liquid-gas transitions. It permits one to scale properties of one liquid to predict those of another.[16] It is likely that it is also valid to some extent for electron-hole liquids as well. To use it in the hydrodynamic model, define scaled variables $\tilde{\mu}$, $\tilde{n}$, and $\tilde{r}$ by $\mu=\tilde{\mu}k_BT_c$, $n=n_c\tilde{n}$, $r=\tilde{r}(Kn_c/k_BT_c)^{1/2}$, and $u=(\tilde{u}/\tau)(Kn_c/k_BT_c)^{1/2}$, where T_c is the critical temperature and n_c the critical density. Then Eq. (17) becomes

$$\frac{d^2\tilde{n}}{d\tilde{r}^2}+\frac{2}{\tilde{r}}\frac{d\tilde{n}}{d\tilde{r}}=\tilde{\mu}(n)-\tilde{\mu}(\bar{n})+\xi\left(\frac{\tilde{u}^2}{2}-\beta\tau\int_{\tilde{r}}^\infty \tilde{u}\,d\tilde{r}\right), \tag{18}$$

where $\xi \equiv mKn_c/\tau^2(k_BT_c)^2$. An alternative scaling is given by $r=\tilde{r}\tau(k_BT_c/m)^{1/2}$ and $u=\tilde{u}(k_BT_c/m)^{1/2}$. Then Eq. (17) would read

$$\xi\left(\frac{d^2\tilde{n}}{d\tilde{r}^2}+\frac{2}{\tilde{r}}\frac{d\tilde{n}}{d\tilde{r}}\right)=\tilde{\mu}(n)-\tilde{\mu}(\bar{n})+\frac{\tilde{u}^2}{2}-\beta\tau\int_{\tilde{r}}^\infty \tilde{u}\,d\tilde{r} . \tag{19}$$

Clearly, if ξ were a small parameter it would justify the consideration of limits where either K or $1/\tau$ were neglected or, equivalently, where

TABLE I. Estimates of parameters of electron-hole liquids in semiconductors.

	$m(m_0)$	σ (erg/cm^2)	τ (sec)	T_c (°K)	n_c (cm^{-3})	$x^2\xi$	$\bar{r}$ (cm)	T_{0H} [a] (°K)	T_{0NK} [b] (°K)
Ge	0.335	2×10^{-4} [c]	4×10^{-5} [d]	6.5 [e]	0.8×10^{17} [e]	1.6×10^{-15}	2.8×10^{-6}	1.4	1.5
Si	0.46	4.8×10^{-3} [f]	1.27×10^{-7} [g]	27 [h]	1.1×10^{18} [h]	9.4×10^{-12}	1.2×10^{-6}	7.8	9
GaP	0.93	1.05×10^{-2} [f]	3.5×10^{-8} [j]	40 [i]	2×10^{18} [i]	1.9×10^{-8}	9.4×10^{-7}	16	20
CdS	1.56	7.2×10^{-3} [f]	10^{-9} [j]	55 [j]	0.7×10^{18} [k]	3.4×10^{-7}	1.4×10^{-6}	26	34
CdSe [l]	0.86	3.1×10^{-4} [f]	10^{-9} [f]	7.3 [f]	1.3×10^{17} [f]	4.0×10^{-6}	2.4×10^{-6}	4.1	5.6
GaAs [m,n]	0.57	?	10^{-10} [j]	?	?	?			

[a] From Eq. (48).
[b] From Eq. (E6).
[c] See T. M. Rice *et al.* (Ref. 1).
[d] C. Benoit à la Guillaume *et al.* (Ref. 22).
[e] G. A. Thomas *et al.* (Ref. 20).
[f] Guessed at by dimensional arguments.
[g] W. Schmid (Ref. 24).
[h] J. Shah *et al.* (Ref. 23).
[i] J. Shah *et al.* (Ref. 25).
[j] R. Leheny *et al.* (Ref. 26).
[k] T. L. Reinecke (Ref. 27).
[l] Used data of R. Leheny *et al.* (Ref. 28).
[m] J. Shah *et al.* (Ref. 29).
[n] O. Hildebrand *et al.* (Ref. 30).

the quantities in brackets in (18) and (19) were neglected. That this is indeed the case for real electron-hole liquids will be discussed below and in Table I.

It is useful to convert other important quantities to scaled units. The surface tension from Eq. (5) in the units of Eq. (18) reads

$$\sigma = K^{1/2} n_c^{3/2} (kT_c)^{1/2} x \,, \tag{20}$$

where x is a dimensionless number

$$x \equiv \int_{-\infty}^{\infty} \left(\frac{d\tilde{n}}{d\tilde{r}}\right)^2 d\tilde{r} \,. \tag{21}$$

One expects that x is a number on the order of one at $T = 0$ °K. For the model equation of state in Appendix A one may analytically show that for $T = 0$ °K, x lies between 5.30 (for $c/a \to 0$) and 2.4 (for $c/a \to 1$). The quantity $x^2\xi = m\sigma^2/\tau^2(kT_c)^3 n_c^2$ can be evaluated in terms of measureable quantities. The width of the interface profile in scaled units is

$$\tilde{w} = (\tilde{n}_l - \tilde{n}_g)^2/x \,.$$

For the model equation of state it lies between 1.7 and 3.7 at $T = 0$ °K.

The hydrodynamic model presented in this paper can be used in making semiquantitative predictions using the same parameters as those of nucleation kinetics. However, some words of caution are in order. In direct-gap materials photon transport of nonequilibrium carriers (polaritons) can result in a particle lifetime which depends on sample thickness.[18] Also stimulated recombination can shorten the lifetime within droplets. Even in indirect-gap materials, the quantitative predictions depend to some extent on the equation of state as we have just illustrated. An accurate equation of state should describe the critical point correctly[19] and the Fermi-liquid behavior at low temperatures[20] and interpolate correctly into the low-density region. To the author's knowledge, no equations of state which satisfy all these requirements have been proposed in the literature. Other requirements for quantitative predictions may include the generalization of hydrodynamics to a two-component anisotropic fluid, estimates of transport coefficients, allowing the lifetime τ to be density dependent, and inclusion of other nonequilibrium effects such as interaction with phonons generated by recombination and thermalization. To the extent that these effects are included the corresponding hydrodynamic model becomes more complex.

All of the numerical results to be presented below are expressed in units of n_c, $k_B T_c$, and $(Kn_c/k_B T_c)^{1/2}$.

In Table I are presented rough estimates of the relevant parameters for the electron-hole liquids in various unstrained semiconductors which have been studied to date. Where the parameters have not been measured, they have simply been guessed at using dimensional arguments. Therefore, the values in particular for direct-gap materials are not to be taken too seriously. The materials are arranged in order of increasing $x^2\xi$. It is to be noted that $x^2\xi$ is orders of magnitude less than one for all the materials in which an electron-hole phase transition has been shown. The question marks for GaAs reflect the uncertainty about a phase transition in this material. Also tabulated in Table I is $\bar{r} = \sigma/(kT_c)n_c$ which sets a distance scale of the interface width for these materials. In addition, predicted values of characteristic temperature T_0 for the hydrodynamic model (T_0^H) and for nucleation kinetics (T_0^{NK}) are given as calculated from Eq. (48) and Eq. (E6), respectively. T_0 is the temperature where the minimum supersaturation equals one and below which significant

departures from equilibrium liquid-gas behavior must occur.

III. DROPLET SOLUTIONS IN THE $\sigma \to 0$ LIMIT

Droplet solutions in the $1/\tau \to 0$ limit have been considered already in Sec. II A. They correspond to critical droplets. Justification for consideration of the other limit of $\sigma \to 0$, or $K \to 0$, was presented in Sec. II D. Then Eq. (17) is

$$\frac{mu^2}{2} - \int_r^\infty m\beta u\, dr = \mu(\bar{n}) - \mu(n). \tag{23}$$

Since flow is to be into the droplet, the velocity u is negative and the left-hand side is positive definite. The right-hand side is negative for values of n between $\bar{n}$ and the high-density metastable region. Therefore, droplet solutions in the $\sigma \to 0$ limit cannot be continuous functions of radius r.

The equations

$$\frac{dn}{dr} = \left[\frac{2mu^2}{r} + \frac{mu}{\tau}\left(1 - \frac{\bar{n}}{n} - \beta\tau\right)\right] \Big/ \left(\frac{d\mu}{dn} - \frac{mu^2}{n}\right) \tag{24}$$

and

$$\frac{du}{dr} = -\frac{1}{mu}\frac{d\mu}{dn}\frac{dn}{dr} - \beta \tag{25}$$

are equivalent to (16) and (17) in the $K \to 0$ limit. One can integrate these outward from $r = 0$ with $n_0 = n(0)$ in the high-density metastable or stable region and $u(0) = 0$. At some "surface" radius r_s where the density is n_+ and u_+, a discontinuous jump will occur to a new density n_- in the low-density metastable region and a new velocity u_-. The problem is the relation of n_- and u_- to n_+ and u_+ and of r_s to $\bar{n}$.

First, the total flux of particles into the droplet should be equal on both sides of the surface. Therefore, we have

$$n_+ u_+ = n_- u_- . \tag{26}$$

Second, using (23) and (26), one must have

$$\frac{mn_+^2 u_+^2}{2n_-^2} + \int_0^{r_s} m\beta u = \mu(n_0) - \mu(n_-), \tag{27}$$

which is the second equation needed to specify n_- and u_- in terms of n_+ and u_+.

Finally, the surface radius r_s may be determined by making a requirement that the discontinuous solutions obtained in the $K \to 0$ limit pass smoothly into continuous solutions for nonzero K. If one multiplies (23) by dn/dr it should be possible to integrate across the surface region. In addition from (26) n^2u^2 is constant across the surface region. Thus one obtains

$$\frac{mn^2u^2}{2}\left(-\frac{1}{n_-} + \frac{1}{n_+}\right) - (n_- - n_+)\int_{r_s}^\infty m\beta u\, dr = (n_- - n_+)\mu(\bar{n}) - f(n_-) + f(n_+). \tag{28}$$

Considerable manipulation of this equation is required to put it in a form where its content is manifest. The details of these manipulations are reserved to Appendix B, but the result is

$$p(n_0) - p(n_D) = \int_0^{r_s} dr\left(\frac{1}{n_-(r)} - \frac{1}{n_+(r)}\right)\frac{d}{dr}\left(\frac{mn_+^2u_+^2}{2}\right) - \int_0^{r_s}(n_- - n_+)m\beta u_+, \tag{29}$$

where n_D is a density in the low-density metastable region defined by $\mu(n_D) = \mu(n_0)$. Here, n_+ is a solution of (24) and (25), and $n_-(r)$ is defined in terms of $n_+(r)$ by (26) and (27). For a more complete discussion, see Appendix B.

Consider the $\beta \to 0$ limit of this equation. The effect of nonzero β is considered in Appendix C. Then from (23) n_0 is fixed by $\mu(n_0) = \mu(\bar{n})$, and therefore $n_D = \bar{n}$. Since $n_- < n_+$ and the second term in (29) is zero, the right-hand side of (29) is positive definite. The left-hand side of (29) is positive only for $\bar{n} > n_g$. Therefore, droplet solutions of the hydrodynamic equations exist only for $\bar{n} > n_g$. The radius r_s is zero at the coexistence curve and increases with supersaturation. Further, the density at the droplet center n_0 increases with supersaturation $S \equiv \bar{n}/n_g - 1$.

An analytic approximation to the droplet size may be obtained from (29) as follows for $n_g \ll n_l$. Then $n_- < \bar{n} \ll n_+$ and n is almost constant for $r < r_s$. Therefore ($r < r_s$)

$$nu = -\frac{1}{4\pi r^2}\int_0^r \left(\frac{n - \bar{n}}{\tau}\right) 4\pi r'^2\, dr' \simeq -\frac{n_0 r}{3\tau}. \tag{30}$$

The right-hand side of (29) may be approximated by setting $n_-(r)$ in the integrand equal to $\bar{n}$. Then

$$p(n_0) - p(\bar{n}) \simeq \frac{mn_0^2 r_s^2}{18\bar{n}\tau^2}. \tag{31}$$

Then to first order in $\bar{n} - n_g$,

$$r_s \simeq \tau\left(\frac{18n_g}{n_l m}\frac{d\mu}{dn}\bigg|_{n_g}(\bar{n} - n_g)\right)^{1/2}, \tag{32}$$

so that the droplet size starts at zero at $\bar{n} = n_g$ and increases with supersaturation.

The droplet radius cannot become so large that u_- exceeds the sound velocity. If that happened the denominator of (24) would become singular. This imposes an effective limit

$$r_s \lesssim \frac{n_- 3\tau}{n_0}\left(\frac{n_-}{m}\left.\frac{d\mu}{dn}\right|_{n_-}\right)^{1/2}. \tag{33}$$

Approximating $n_- \simeq \bar{n}$, and using (32), the sound velocity limit is not exceeded at supersaturations $S \equiv \bar{n}/n_g - 1$ given by $S \lesssim n_g/2n_l$. At higher supersaturations r_s is determined by (33). [Note that in the ideal-gas limit the approximation (31) is unnecessary, for (29) can be evaluated exactly. This gives $S \lesssim 0.213 n_g/n_l$, and $r_s \lesssim 3\tau\bar{n}/n_l(kT/em)^{1/2}$, where $e = 2.718\ldots$. This upper limit on r_s differs from the result of nucleation kinetics for "stable droplets" given in Appendix E by $(2\pi/e)^{1/2}$. Further $n_- > e^{-1/2}\bar{n}$.]

A qualitative characterization of these droplet solutions in the $\sigma \to 0$ and $\beta \to 0$ limit is as follows. The density at droplet center n_0 exceeds n_l by an amount which increases with supersaturation. The density decreases slightly and the velocity increases linearly with radius until the surface r_s is reached. At the surface there is a discontinuous jump to a lower density $n_- < \bar{n}$ and a much higher velocity u_-. For $r \gg r_s$ the density increases toward $\bar{n}$ as $n - \bar{n} \propto r^{-4}$, and the velocity goes to zero as $u \sim r^{-2}$. This may be seen by linearizing (23) in the $\beta \to 0$ limit about $\bar{n}$. Therefore, the total flux of particles into the droplet from infinity is nonzero! Numerical studies which have been carried out show that typically the total flux from infinity is a sizeable fraction of the total flux at $r \simeq r_s$.

This rather pathological behavior at infinity can be corrected in two ways with generally negligible effects on droplet properties as calculated from Eq. (29). First, for nonzero β one may show that n must approach $\bar{n}$ exponentially for $r \gg r_s$ with decay constant $[m\beta/(\tau\bar{n}d\mu/d\bar{n})]^{1/2}$. An analysis of the effect of β presented in Appendix C shows that for values of a characteristic parameter $\eta < 1$, where η is defined as $\eta \equiv 6\beta\tau n_g/n_l$ the droplet properties differ negligibly from (29) but the net flux from infinity is zero. For $\eta \gtrsim 1$, and therefore temperatures near T_c, the friction coefficient is an important correction to droplet properties. Second, in the presence of a finite density of droplets, the net flux from infinity must be zero. This is discussed in terms of a "cell model" presented in Appendix D. As in nucleation kinetics, we term these droplet solutions "stable" droplets.

IV. ISOLATED-DROPLET SOLUTIONS OF THE COMPLETE EQUATIONS

It is clear from Secs. I–III that the properties of critical droplets (Sec. II A) and stable droplets (Sec. III) are quite distinct. The radius r_s of critical droplets starts at infinity at $\bar{n} = n_g$ and decreases toward zero with increasing supersaturation. The radius of stable droplets start at zero at $\bar{n} = n_g$ and increases with supersaturation. Both these limits correspond to $\xi = 0$ as discussed in Sec. II D.

In this section, isolated-droplet solutions for nonzero ξ are obtained. Appendix D discusses a "cell model" for interacting droplets.

A. Numerical solution

One way to study $\xi \neq 0$ is by straightforward numerical integration of (16) and (17). This has been carried out by guessing n_0 and integrating outward using a prediction-corrector method. If the solutions do not converge toward $\bar{n}$ as $r \to \infty$, a new n_0 is guessed at and the integration repeated. It is found that above a minimum supersaturation, droplet solutions corresponding to both small r_s (critical droplets) and large r_s (stable droplets) can be found. This is illustrated in Fig. 2 for $\beta = 0$ and $\xi = 5 \times 10^{-4}$. With increasing supersaturation these solutions approach the $\xi \to 0$ limit solutions discussed previously. Note that the discontinuous interface and velocity profile of Sec. III has been replaced by a continuous transition from high to low densities and low to high velocities.

In practice, this procedure is difficult to carry out for very small ξ because the left-hand side of (17) is found to be negligible compared to the terms on the right-hand side except in the interface region. These numerical results suggest an analytic approximation which takes advantage of the smallness of ξ for the electron-hole liquids which have been studied to date.

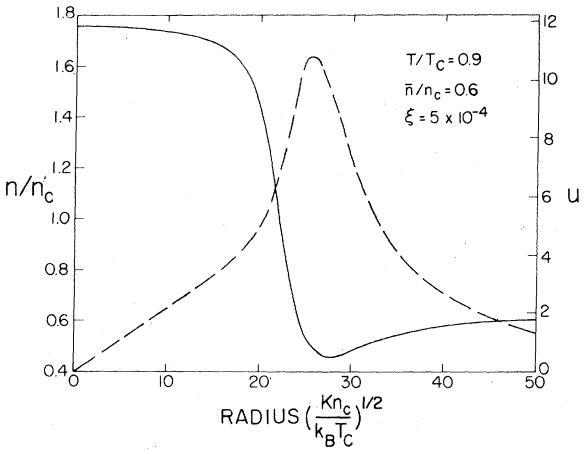

FIG. 2. Density profile (solid) and velocity profile (dashed) for stable droplet at $\bar{n}/n_c = 0.6$, $T/T_c = 0.9$, $\xi = 5 \times 10^{-4}$. Note that the density at droplet center n_0 exceeds $n_{\mathrm{liq}} = 1.63 n_c$. The gas coexistence curve is $n_{\mathrm{gas}} = 0.453 n_c$.

B. $r_s/W \gg 1$ approximation

The principal assumption of the following analytic treatment is that the interface width, as given by Eq. (6), is smaller than or comparable to the droplet radius r_s. To estimate when this is valid, use Eqs. (9) and (31) to determine that critical and stable droplets become equal in size at $\tilde{r}_s^3 = 36\tilde{\bar{n}}x/\tilde{n}_0^2\xi$ in the scaled units of Sec. II D, at a supersaturation given by $\tilde{p}(n_0) - \tilde{p}(\bar{n}) \cong (2\tilde{n}_0^2\xi x^2/9\tilde{\bar{n}})^{1/3}$. Since $\tilde{\bar{n}} \gtrsim \tilde{n}_g$ and $\tilde{n}_0 \simeq \tilde{n}_l$, it is clear that $36\tilde{n}_g x^4/\tilde{n}_l^8\xi \gtrsim 1$ is required. Since $\xi \ll 1$ for all electron-hole liquids studied to date, one is assured that this assumption will be valid for some range of temperatures bounded on one side by $\tilde{T}_c = 1$.

The assumed narrowness of the interface width compared to r_s means that: (i) K can be ignored except in the interface region so that (24) and (25) are valid outside this region, (ii) quantities such as nu and $\int_0^r m\beta u$ are constant through the interface region, and (iii) the $(2K/r)(dn/dr)$ term can be dropped in calculating the interface density and velocity profile. Then the interface equation is given by

$$\frac{Kd^2n}{dr^2} \simeq \frac{m(n^2u^2)}{2n^2} + \mu(n) - \mu(n_0) + \int_0^{r_s} m\beta u. \tag{34}$$

This may be integrated to give

$$K\int_{r_+}^{r_-}\left(\frac{dn}{dr}\right)^2 dr \simeq K\int_{n_+}^{n_-} dn \left\{\frac{2}{K}\left[\frac{m(nu)^2}{2}\left(-\frac{1}{n}+\frac{1}{n_+}\right) - p(n) + p(n_+) - n[\mu(r_s)-\mu(n)] + n_+[\mu(r_s)-\mu(n_+)]\right]\right\}^{1/2} \tag{35}$$

where n_- is chosen to match on to a solution of (24). This condition on n_- requires that u_- cannot exceed the sound velocity. Here $\mu(r_s) \equiv \mu(n_0) = \int_0^r m\beta u\, dr$. Note that Eq. (35) is not identical to the corresponding Eq. (5) for a plane interface in the $1/\tau \to 0$ limit. Therefore, setting this integral equal to the surface tension for a plane interface is a rough approximation which is best for small ξ. Note further that approximation (iii) above can be removed by iteration.

Multiplying (17) by dn/dr and integrating according to the procedures used for obtaining Eqs. (29) and (31), as given in Appendix B, leads to the relation

$$p(n_0) - p(n_D) \simeq \frac{2K}{r_s}\int_{r_+}^{r_-}\left(\frac{dn}{dr}\right)^2 dr + \int_0^{r_s} dr\left(\frac{1}{n_-}-\frac{1}{n_+}\right)\frac{d}{dr}\left(\frac{mn_+^2u_+^2}{2}\right) - \int_0^{r_s}(n_- - n_+)m\beta u_+ + \frac{K}{2}\left(\frac{dn}{dr}\right)^2\Bigg|_{r_-} - \frac{K}{2}\left(\frac{dn}{dr}\right)^2\Bigg|_{r_+} \tag{36}$$

Here $\mu(n_0) = \mu(n_D)$ and $\mu(n_0) = \mu(\bar{n}) + \int_0^\infty m\beta u$. In the rest of this section the consequences of Eq. (36) will be discussed in detail for the $\beta \to 0$ limit. The treatment of nonzero β is presented in Appendix C, as discussed in Sec. III.

For $\beta \to 0$, $n_D = \bar{n}$, and the left-hand side of this equation is positive for $\bar{n} > n_g$. The right-hand side is manifestly positive definite. The first term is large at small r_s. The second term again varies as $mr_s^2n_0^2/18\tau^2\bar{n}$. The third term is zero since $\beta \to 0$ is assumed. The fourth term according to (24) diverges as the droplet size grows large enough for u_- to approach the sound velocity. The fifth term is negligible for $\xi \ll 1$. Hence, the right-hand side is large at small r_s and large r_s and has a positive minimum somewhere between. Thus, a minimum supersaturation $\bar{n}_{\min} > n_g$ or $S_{\min} > 0$ is required for the existence of droplets. Above this minimum stationary solutions corresponding to both critical (small r_s) and stable droplets (large r_s) are found.

C. Approximate analysis for isolated droplet properties

Simple formulas for the minimum stable radius, minimum supersaturation, and droplet properties as a function of supersaturation can be obtained by the substitution for Eq. (36)

$$p(n_0) - p(\bar{n}) \simeq \frac{2\sigma}{r_s}Z(T) + \frac{mr_s^2n_0^2}{18\tau^2\bar{n}} + \delta(r_s - 3\tau\bar{n}c(\bar{n})/n_0), \tag{37}$$

where the last term is a δ function of the argument. Here σ is the $T = 0\,^\circ$K value of the surface tension, and the surface tension at finite T is $\sigma(T) = \sigma z(T)$. Clearly $z(T) \to 0$ as $T \to T_c$. The second term again corresponds to an assumption that n_- does not differ appreciably from $\bar{n}$ (this will be removed later). The third term corresponds to the fourth term in (36) which limits the velocity to less than the sound velocity $c(n) = [(nd\mu/dn)/m]^{1/2}$. Solution of (37) can be divided into two regimes depending on whether the minimum of the sum of the first two terms corresponds to an r_s less than or more than the sound velocity limit.

In the first case, (37) is a cubic equation for r_s whose two positive solutions are expressed in terms of

$$\cos\phi = -zx(3\xi\tilde{n}_0^2/2\tilde{\bar{n}})^{1/2}\,[\tilde{p}(n_0) - \tilde{p}(\bar{n})]^{-3/2}, \tag{38}$$

where $\pi > \phi > \frac{1}{2}\pi$. Then the solutions for $\tilde{r}_s$ are

$$\tilde{r}_s = \left(\frac{24\tilde{\bar{n}}}{\tilde{n}_0^2\xi}[\tilde{p}(n_0)-\tilde{p}(\bar{n})]\right)^{1/2}\left[\cos\frac{\phi}{3};\cos\left(\frac{\phi}{3}+\frac{4\pi}{3}\right)\right]. \tag{39}$$

Here the $\cos\frac{1}{3}\phi$ solution corresponds to stable droplets (large $\tilde{r}_s$), and the $\cos(\frac{1}{3}\phi+\frac{4}{3}\pi)$ to critical droplets (small $\tilde{r}_s$). These solutions are equal at a minimum supersaturation

$$\tilde{p}(n_0)-\tilde{p}(\bar{n}) = (\tfrac{3}{2}\xi z^2 x^2 \tilde{n}_0^2/\tilde{\bar{n}})^{1/3} \tag{40}$$

and a minimum stable radius

$$\tilde{r}_s \simeq (18\tilde{\bar{n}}zx/\tilde{n}_0^2\xi)^{1/3}. \tag{41}$$

In conventional units these equations read

$$p(n_0)-p(\bar{n}) = (3z^2 m\sigma^2 n_0^2/2\tau^2\bar{n})^{1/3} \tag{40'}$$

and

$$r_s = (18\tau^2\sigma\bar{n}z/mn_0^2)^{1/3}. \tag{41'}$$

In the second case, in the scaled units defined by Sec. II C and $c=\tilde{c}(kT_c/m)^{1/2}$, the minimum radius and minimum supersaturation are determined by

$$\tilde{r}_s = 3\tilde{\bar{n}}\tilde{c}/\xi^{1/2}\tilde{n}_0 \tag{42}$$

and

$$\tilde{p}(n_0)-\tilde{p}(\bar{n}) \simeq 2\xi^{1/2}zx\tilde{n}_0/3\tilde{\bar{n}}\tilde{c}+\tfrac{1}{2}\tilde{\bar{n}}\tilde{c}^2. \tag{43}$$

Note that $\tilde{c}<1$ and in the ideal-gas limit $\tilde{c}\simeq\tilde{T}^{1/2}$. In conventional units these equations read

$$r_s = 3\tau\bar{n}c(\bar{n})/n_0 \tag{42'}$$

and

$$p(n_0)-p(\bar{n}) = 2\sigma z/3\tau\bar{n}c+\tfrac{1}{2}mc^2\bar{n}. \tag{43'}$$

Define a temperature $\tilde{T}^*$ by where (41) and (42) become equal, and assume the supersaturation $S=(n-n_g)/n_g$ is small. Then T^* is defined by

$$\tilde{n}_g \simeq (\xi^{1/4}\tilde{n}_l^{1/2}z^{1/2}x^{1/2}/\tilde{c}^{3/2})(\tfrac{2}{3})^{1/2}. \tag{44}$$

Then for $\tilde{T}>\tilde{T}^*$, Eqs. (40) and (41) are applicable, and for $\tilde{T}<\tilde{T}^*$, Eqs. (42) and (43) are applicable. For $\tilde{T}>\tilde{T}^*$

$$S \simeq (3\xi^2 z^2 x^2/\tilde{n}_l\tilde{c}^6 2\tilde{n}_g)^{1/3} \tag{45}$$

so that $S\propto\exp(+\Phi_\infty/3kT)$ and $\tilde{r}_s\propto\exp(-\Phi_\infty/3kT)$, where Φ_∞ is the work function of the infinite liquid. At $T=T^*$

$$\tilde{p}(n_0)-\tilde{p}(\bar{n}) \simeq [\xi^{1/2}\tilde{n}_l\tilde{c}zx(\tfrac{3}{2})]^{1/2}. \tag{46}$$

For $\xi\ll 1$ the right-hand side of (46) is much less than one, which is consistent with the initial assumption that $S\ll 1$.

The minimum supersaturation, $S_{\min}$ remains less than one for $\tilde{T}_0<\tilde{T}<T^*$ so that

$$\tilde{p}(n_0)-\tilde{p}(\bar{n}) \simeq \tilde{n}_l\frac{d\mu}{d\tilde{n}}(\tilde{\bar{n}}-\tilde{n}_g). \tag{47}$$

Here $\tilde{T}_0$ is defined by $S_{\min}=1$, and $S_{\min}$ is given approximately by

$$S_{\min} \simeq 2\xi^{1/2}zx/3\tilde{n}_g\tilde{c}^3+\tilde{n}_g/2\tilde{n}_l \tag{48}$$

for $\tilde{T}_0\lesssim\tilde{T}\lesssim T^*$. In this region $\tilde{r}_s\propto\tilde{n}_g\simeq\exp(-\Phi_\infty/kT)$ for an ideal gas. Equation (48) should be compared with the nucleation kinetics result (E1). Note that $\tilde{T}_0$ is comparable in both theories and, in the ideal gas limit, depends on the same combination of variables $\xi^{1/2}/\tilde{n}_g\tilde{T}^{3/2}$. However, the detailed dependence on temperature of the minimum stable $\tilde{r}_s$ and minimum supersaturation $\tilde{S}_{\min}$ are quite different in the two theories.

With increasing supersaturation, according to (38) and (39), critical droplets get smaller and tend toward the τ-independent droplets of Sec. II A. Stable droplets get larger and tend toward the σ-independent droplets of Sec. III. The sound velocity limit on stable droplet size is reached at a supersaturation $S\simeq\tilde{n}_g/2\tilde{n}_l$.

D. Isolated droplet solutions near the spinodal line

As $\bar{n}$ approaches the spinodal line $\tilde{c}$ tends toward zero and (37) would predict that $\tilde{r}_s$ would go toward zero. This conclusion is spurious and an artifact of the approximation (37) to the more general equation (36). Equation (37) assumes that n_- does not depart significantly from $\bar{n}$.

To see what happens near the spinodal line, expand $\mu(n)$ about the spinodal

$$\mu(n) \simeq \mu(n_s)+\frac{1}{2}\left.\frac{d^2\mu}{dn^2}\right|_{n_s}(n-n_s)^2, \tag{49}$$

set r_s to the value determined by the sound velocity limit

$$u^2 \simeq \frac{n_0^2 r_s^2}{9\tau^2 n_-^2} \simeq c^2 = \frac{n_-}{2m}\left.\frac{d^2\mu}{dn^2}\right|_{n_s}(n_- - n_s), \tag{50}$$

and plug into (21). This gives

$$n_- - n_s = -\tfrac{1}{6}n_s - \tfrac{1}{2}[\tfrac{1}{9}n_s^2+\tfrac{8}{3}(\bar{n}-n_s)^2]^{1/2}. \tag{51}$$

As $\bar{n}\to n_s$, $n_-\to\frac{2}{3}n_s$, and one may show from (50) and (51) that r_s increases monotonically as $\bar{n}\to n_s$. The maximum isolated stable droplet size is then approximately

$$r_s \lesssim \left(\frac{4n_s^4\tau^2}{3mn_0^2}\left.\frac{d^2\mu}{dn^2}\right|_{n_s}\right)^{1/2} = r_s^{\max}. \tag{52}$$

As $T \to 0$, $n_s \to 0$, and, consequently, so does $r_s^{\max}$.

An argument against the stability of isolated droplet solutions for $\bar{n} > n_s$ is as follows. A linear analysis of (14) and (15) shows that the frequency of density fluctuations of wavelength $1/k$ is

$$\omega = \tfrac{1}{2}i\left(\beta + \frac{1}{\tau} \pm \frac{1}{2}\right)\left[-\left(\beta - \frac{1}{\tau}\right)^2 + \frac{4\bar{n}k^2}{m}\left(\frac{d\mu}{dn} + Kk^2\right)\right]^{1/2}. \tag{53}$$

Inside the spinodal line $d\mu/dn$ is negative, and fluctuations for k in the range $-(\beta m/\tau\bar{n})(d\mu/dn) \lesssim k^2 \lesssim -(1/K)(d\mu/dn)$ grow exponentially with time. For a scaled $\tilde{k}$ defined by $k = \tilde{k}(kT_c/Kn_c)^{1/2}$ this is equivalently $-\beta\tau\xi/(\tilde{n}d\tilde{\mu}/d\tilde{n}) \lesssim \tilde{k}^2 \lesssim -d\tilde{\mu}/d\tilde{n}$. Thus, the smallness of ξ implies that most of the spinodal region is unstable.

While isolated droplet solutions cannot be stable for $\bar{n}$ inside the spinodal (unstable) region, interacting droplet solutions do exist. A "cell model" for their properties is presented in Appendix D. This model does not alter the conclusion that as $T \to 0$ the droplet size must go toward zero. The behavior of critical droplets as $\bar{n}$ approaches n_s is the same as in the theory of Cahn and Hilliard.[11,13]

E. Statistical fluctuations and the low-temperature region $\tilde{T} < \tilde{T}_0$

Nucleation and decay rates could presumably be derived within the context of the hydrodynamic model by adding statistical fluctuations to the equations.[14] While this calculation has not been performed, let us assume that the conclusions are similar to those of nucleation kinetics.[6,7] These are that (a) the smaller the difference in size between critical and stable droplets the faster the decay rate, (b) the smaller the critical droplet size the faster the nucleation rate, and (c) for $\tilde{T} > \tilde{T}_0$ regions of excitation $\bar{n}$ can be found where neither nucleation or decay rates are large so that a metastable state can exist.

At $\tilde{T} < \tilde{T}_0$ the assumptions of the nucleation kinetics model fail. First, the assumption of an ideal-gas phase fails since, within the context of the model, the concentration of dimers, trimers, etc., become comparable to those of monomers. Second, the assumption of ascribing macroscopic properties, such as surface tension, to critical droplets fails since the droplets contain only a few particles.

In the hydrodynamic model, at $\tilde{T} < \tilde{T}_0$ the ratio of the maximum critical size to the interface width according to (42) and (45) is bounded by $\tilde{r}_s/\tilde{w} \lesssim 2x^2/\tilde{n}_l^3\tilde{c}^2$, which is a number around one. Thus, at low temperatures the conditions for application of the approximations of Sec. IV B to critical droplets are invalid. Solutions for critical droplets might presumably be obtained numerically as in Sec. IV A. However, the effect of statistical fluctuations is almost certain to make the properties of these solutions unimportant. Estimates of the number of particles in a maximum critical droplet are easily obtained using the parameters listed in Table I. The critical droplets are so small ($N < 100$) that they do not act as a barrier to nucleation and decay.

The hydrodynamic model does not require an assumption of an ideal-gas phase. Hence it continues to predict the existence and properties of isolated stable droplets in the $\tilde{T} < \tilde{T}_0$ region. A gas density $\bar{n} \geq \xi^{1/2}\tilde{n}_l^3/3\tau x$ is required for the assumptions of Sec. IV B to be valid and, probably, also for stable droplets to have a reasonably long lifetime against statistical fluctuations. The hydrodynamic model also predicts a region of absolute instability in the phase diagram for $\bar{n}$ greater than the spinodal line n_s. This prediction is incompatible with the low-temperature phase diagram suggested by Combescot and Combescot.[21]

V. CONCLUSIONS

A hydrodynamic model has been presented for condensation in systems of finite-lifetime particles such as electrons and holes in semiconductors. It is a natural extension of the theories of critical droplets and spinodal decomposition for ordinary phase transitions developed by Cahn and Hilliard. It is an alternative theory to nucleation kinetics which has the advantages of incorporating transport effects, of being applicable to nonideal-gas phases, and of predicting rather than postulating droplet properties. In particular, the capillarity approximation used in nucleation kinetics is a consequence of the hydrodynamic model for critical droplets but is not correct for the stable droplets which are unique to electron-hole condensation.

An approximate analysis of stationary-droplet properties was presented which took advantage of the smallness for real electron-hole liquids of a dimensionless parameter ξ upon which both hydrodynamics and nucleation kinetics depend. The droplets are characterized by a velocity as well as a density profile. The velocity is maximum and the density a minimum just outside the droplet surface, even for negligible scattering from impurities or phonons. This leads to quantitative differences between hydrodynamics and the capillarity

approximation commonly used in nucleation kinetics. A fundamental limit on the droplet size is imposed by a requirement that the velocity does not exceed the sound velocity. The kinetic energy contribution to the Gibbs free energy is quite significant. However, stable droplets do not correspond to extrema of any kind of "generalized Gibbs free energy" as they do in nucleation kinetics. The internal properties of droplets such as density and chemical potential are weakly dependent on the supersaturation.

The hydrodynamic model is characterized by temperature ranges where particular physical effects are dominant. For temperatures greater than that where $6\beta\tau n_g/n_l = 1$, where β is an inverse scattering time, the scattering modifies droplet properties substantially. For temperatures less than that defined by (44), the sound-velocity limit determines the minimum supersaturation and minimum stable radius. For temperatures less than T_0 defined by the minimal supersaturation being equal to one, significant departures from equilibrium liquid-gas behavior must occur. This is well established experimentally in Ge and also appears to be valid in Si. It is remarkable that both nucleation kinetics and hydrodynamics give similar quantitative values for T_0, as presented in Table I. In view of the approximations involved and the uncertainties in data, the differences in the value of T_0 between nucleation kinetics and hydrodynamics are probably not significant. At temperatures much less than T_0, both theories do not allow sizeable stationary-droplet solutions. Nevertheless, spectroscopic evidence suggests that sizeable volumes of electron-hole liquid exist at temperatures well below T_0. Perhaps this can be explained in terms of time-dependent solutions of the hydrodynamic equations.

Other novel features of the hydrodynamics are connected with its applicability to nonideal gases. First, the structure of critical and stable droplets continues to persist up to the critical temperature. Second, a region of absolute instability termed the spinodal region exists, where isolated stable-droplet solutions cannot be found. This is especially important since it rules out a time-independent droplet description of the liquid-gas configuration under uniform steady-state excitation at extremely low temperature ($T \ll T_0$).

This theory in its present form is capable of making quantitative predictions with the same parameters as nucleation kinetics for experimentally accessible quantities such as droplet size, thresholds, number density, chemical potential, etc. Considerable improvement will come with the development of equations of state for electron-hole fluids in semiconductors.

APPENDIX A: PROPERTIES OF THE MODEL EQUATION OF STATE

For the numerical calculations a model equation of state was chosen which contained the essential physics of a first-order phase transition and the advantage of numerical simplicity. In the scaled variables of Eq. (18), it is the modified Van der Waal's equation

$$p = -an^2 + n(T + nc)/(1 - bn)\,. \tag{A1}$$

The term nc is added to allow for a finite compressibility of the liquid phase at $T = 0\,^\circ\mathrm{K}$. In order for $T_c = 1$ and $n_c = 1$, one must have $a = (3b - b^2)^{-1}$, $c = (1 - 3b)/(3b - b^2)$, and $b < \frac{1}{3}$. The chemical potential is

$$\mu = -2an + T\ln\frac{n}{1-bn} + \frac{T+nc}{1-bn} - \frac{c}{b}\ln(1-bn) - T\,. \tag{A2}$$

At $T = 0$ the density of the liquid phase is $3.0 = n_l$ regardless of the ratio c/a. The chemical potential of the liquid phase at $T = 0$ varies between $-3.37 (c/a = 0)$ and $-1.50 (c/a = 1)$. This implies a corresponding density of the gas phase at $T = 0\,^\circ\mathrm{K}$ $n_g \approx e^{+\mu(n_l)/T}$.

The surface-tension integral, Eq. (21), may also be evaluated analytically. One finds that x, defined in Sec. II C, varies between 5.30 (for $c/a \to 0$) and 2.4 (for $c/a \to 1$).

The spinodal line n_s is defined by $d\mu(n_s)/dn = 0$, and is illustrated in Fig. 1. At very low temperatures where $bn_s \ll 1$, $n_s \simeq T/(2a - 2c - 2Tb)$ and so goes to zero as $T \to 0$. Clearly $n_s \gg n_g$ by orders of magnitude except near the critical temperature. Whether this large difference between n_s and n_g is valid for a realistic system depends on the equation of state. For the figures the value $b = 0.233$ corresponding to $c/a = 0.3$ was chosen.

APPENDIX B: DERIVATION OF SUM RULES

In this Appendix details of manipulations which lead to the sum rules (26) and (36) are presented. The starting point is

$$\frac{Kd^2n}{dr^2} + \frac{2K}{r}\frac{dn}{dr} = \frac{mu^2}{2} + \mu(n) - \mu(n_0) + \int_0^r m\beta u\, dr\,. \tag{B1}$$

Consider first the limit $K \to 0$. Because $\mu(n)$ is a triple-valued function below the critical temperature, there can be three types of solutions: (a) in the high-density metastable and stable regions $n_a(r), u_a(r)$; (b) in the unstable region $n_b(r), u_b(r)$; and (c) in the low-density metastable and stable regions $n_c(r), u_c(r)$. For stationary spherical droplets, solutions of type (a) for r less than the

surface radius r_s must be matched on to solutions of type c for $r > r_s$. These solutions may be obtained by integrating (24) and (25) subject to the boundary conditions $n_a(0), u_a(0) = n_0, 0$ and $n_c(\infty), u_c(\infty) = \bar{n}, 0$. The $r = 0$ boundary condition uniquely specifies the solution of type (a). However, the $r = \infty$ boundary condition does not specify the solution of type (c). The type (c) solution must be determined by the matching condition at $r = r_s$. This Appendix is concerned with determining the matching condition and with deriving two relations among the three parameters n_0, $\bar{n}$, and r_s.

Clearly, from (B1), one relation must be given by $I(r_s) = 0$, where

$$I(r_s) \equiv \mu(n_0) - \mu(\bar{n}) - \int_0^{r_s} m\beta u_a(r)\, dr - \int_{r_s}^{\infty} m\beta u_c(r)\, dr . \tag{B2}$$

In order to use this relation one must know which type (c) solution is needed to complete the last integral in (B2). Suppose at a particular choice of n_0, $\bar{n}$, and r_s the higher density and corresponding velocity are $n_+ = n_a(r_s)$ and $u_+ = u_a(r_s)$. In the low-density metastable or stable region another density $n_-(r_s)$ and corresponding velocity $u_-(r_s)$ may be defined as follows. First, the particle fluxes across the surface are equal

$$n_-(r_s)u_-(r_s) = n_+(r_s)u_+(r_s) . \tag{B3}$$

Second, (B1) must be obeyed in the $K \to 0$ limit

$$\frac{mu_-^2}{2} + \mu(n_-) = \mu(n_0) - \int_0^{r_s^+} m\beta u_a(r)\, dr = \frac{mu_+^2}{2} + \mu(n_+) . \tag{B4}$$

Taking $n_c(r_s) = n_-(r_s)$ and $u_c(r_s) = u_-(r_s)$ completely specifies a type (c) solution which may be continued to large $r \gg r_s$. [Note that $dn_-(r_s)/dr_s \neq dn_c(r_s)/dr$ and $du_-(r_s)/dr_{cs} \neq du_c(r_s)/dr$. Rather, they are determined through (B3) and (B4) by dn_a/dr and du_a/dr evaluated at r_s.] These can be used in (B2) by noting that

$$\left.\frac{dI(r_s)}{dr_s}\right|_{n_0,\bar{n}} = -m\beta u_+(r_s) + m\beta u_-(r_s) . \tag{B5}$$

Thus

$$I(r_s) = \mu(n_0) - \mu(\bar{n}) - \int_0^{r_s} m\beta[u_+(r_s') - u_-(r_s')]\, dr_s' , \tag{B6}$$

which has the advantage that it may be evaluated without specifying the type (c) solution.

A second relation may be obtained by multiplying (B1) by dn/dr and integrating across the surface region from $r_+ < r_s$ to $r_- > r_s$. Assume that nu and $\int_r^{\infty} m\beta u\, dr$ are approximately constant across the surface region. Assume further that the left-hand side of (B1) is important only for $r_+ < r < r_-$. It may be verified by numerical solution that these assumptions are valid for $r_s/w \gtrsim 1$. Then using (B4) one finds

$$\frac{K}{2}\left(\frac{dn}{dr}\right)^2\Big|_{r_-} - \frac{K}{2}\left(\frac{dn}{dr}\right)^2\Big|_{r_+} + 2K\int_{r_+}^{r_-}\frac{1}{r}\left(\frac{dn}{dr}\right)^2 dr = mn_+^2u_+^2\left(-\frac{1}{n_-}+\frac{1}{n_+}\right) - p(n_-) + p(n_+) . \tag{B7}$$

To manipulate (B7) into the required form add and subtract $p(n_0) - p(n_D)$ to the right-hand side, where n_D is in the low-density metastable region and defined by $\mu(n_0) = \mu(n_D)$. Further needed relations are first

$$p(n_+) - p(n_0) = \int_0^{r_s} dr_s' \frac{dn_+(r_s')}{dr_s} n_+(r_s')\frac{d\mu}{dn}[n_+(r_s')] , \tag{B8}$$

and a similar relation for $p(n_-) - p(n_D)$. Then the right-hand side of (B7) is

$$J_{\rm rhs} = p(n_0) - p(n_D) + mn_+^2u_+^2\left(-\frac{1}{n_-}+\frac{1}{n_+}\right) + \int_0^{r_s} dr\left(\frac{dn_+'}{dr}n_+'\frac{d\mu(n_+)}{dn_+} - \frac{dn_-'}{dr}n_-'\frac{d\mu(n_-')}{dn_-}\right) . \tag{B9}$$

Take the derivative with respect to r_s. Then

$$\frac{dJ_{\rm rhs}}{dr_s} = \left(-\frac{1}{n_-}+\frac{1}{n_+}\right)\frac{d}{dr_s}(mn_+^2u_+^2) + mn_+^2u_+^2\left(\frac{1}{n_-^2}\frac{dn_-}{dr_s} - \frac{1}{n_+^2}\frac{dn_+}{dr_s}\right) + \frac{dn_+}{dr_s}n_+\frac{d\mu}{dn_+}(n_+) - \frac{dn_-}{dr_s}n_-\frac{d\mu(n_-)}{dn_-} . \tag{B10}$$

From (B4) one has

$$n_-\frac{d\mu}{dn_-}\frac{dn_-}{dr_s} - n_-mu_-^2\frac{dn_-}{dr_s} = \frac{1}{n_-}\frac{d}{dr_s}\left(-\frac{mn_-^2u_-^2}{2}\right) - n_-m\beta u_+ , \tag{B11}$$

and

$$n_+\frac{d\mu}{dn_+}\frac{dn_+}{dr_s} - mu_+^2\frac{dn_+}{dr_s} = \frac{1}{n_+}\frac{d}{dr_s}\left(-\frac{mn_+^2u_+^2}{2}\right) - n_+m\beta u_+ . \tag{B12}$$

[Note that (B11) and (B12) are not symmetric with respect to +, − interchange because $dI(r_s)/dr_s \neq 0$.] One also has from (B3) that $d(n_-^2u_-^2)/dr_s = d(n_+^2u_+^2)/dr_s$. Combining (B10)–(B12), one has

$$\frac{dJ_{\rm rhs}}{dr_s} = \left(-\frac{1}{n_-}+\frac{1}{n_+}\right)\frac{d}{dr_s}\left(\frac{mn_+^2u_+^2}{2}\right) + (n_- - n_+)m\beta u_+ . \tag{B13}$$

Putting (B4) and (B13) together and approximating the $1/r$ in the third term on the left-hand side of (B4) by $1/r_s$, one obtains

$$p(n_0)-p(n_D)=\int_0^{r_s}dr\left(\frac{1}{n_-}-\frac{1}{n_+}\right)\frac{d}{dr}\left(\frac{mn_+^2u_+^2}{2}\right)-\int_0^{r_s}(n_--n_+)m\beta u_+ +\frac{2K}{r_s}\int_{r_+}^{r_-}\left(\frac{dn}{dr}\right)^2dr+\frac{K}{2}\left(\frac{dn}{dr}\right)^2\Big|_{r_-}-\frac{K}{2}\left(\frac{dn}{dr}\right)^2\Big|_{r_+}, \tag{B14}$$

which is the same as (36).

Equations (B6) and (B14) are the essential results. Note that $I(r_s)=0$ and (B14) may be calculated in terms of type (a) solutions which are completely specified by the input values of n_0 and $\bar{n}$. These forms are advantageous because the type (a) solutions are easily approximated for $n_g/n_l \ll 1$. Similar relations may also be derived in terms of type (c) solutions, but they do not lend themselves easily to approximation.

APPENDEX C: EFFECT OF FRICTION COEFFICIENT

In this Appendix, details of the analysis of the effect of the friction term are presented. In practice, the coefficient β will be density and temperature dependent. In addition, there will be other dissipative terms such as viscosity. The analysis here will therefore be indicative of the effect of dissipative terms, but in no way is it meant to be quantitatively compared to experiment. Only the stable droplets of Sec. III will be considered.

The starting point is then the equation for stable droplets

$$0=\frac{mu^2}{2}+\mu(n)-\mu(\bar{n})-\int_r^\infty m\beta u\,dr, \tag{C1}$$

where

$$\mu(n_D)=\mu(\bar{n})+\int_0^\infty m\beta u\,dr, \tag{C2}$$

and $\mu(n_0)=\mu(n_D)$. The key to the analysis is to consider limits of (C1) where either the first term $\frac{1}{2}mu^2$ or the fourth term $\int_r^\infty m\beta u$ is negligible. Solutions of this equation in these limits will then be joined at an appropriate point for a complete description. Throughout the following treatment it will be assumed that $n_l \gg n_g$, that one can linearize about $\bar{n}$ for $r>r_s$, and that n varies little from n_0 for $r<r_s$.

First, in the limit $\frac{1}{2}mu^2$ negligible, begin by differentiating (C1) with respect to r to obtain

$$m\beta u=-\frac{\partial\mu}{\partial n}\frac{dn}{dr}. \tag{C3}$$

Then use (16) and differentiate again to obtain

$$-\frac{1}{4\pi r^2}\frac{d}{dr}\left(4\pi r^2 n\frac{\partial\mu}{\partial n}\frac{dn}{dr}\right)+\frac{m\beta}{\tau}(n-\bar{n})=0. \tag{C4}$$

For an ideal gas $\bar{n}d\mu/d\bar{n}$ is independent of n. In the spirit of being able to linearize about $\bar{n}$ we take $n(d\mu/dn)\cong n(d\mu/d\bar{n})$ even in nonideal-gas regions. Then the solution of (C4) which approaches $\bar{n}$ at large $r\gg r_s$ is

$$n-\bar{n}=(A/r)e^{-\lambda r};\qquad \lambda^2=m\beta/\tau\bar{n}d\mu/d\bar{n}. \tag{C5}$$

Note that (C3) imposes a definite relation between u and $n-\bar{n}$, i.e.,

$$\frac{u}{n-n}=\frac{1}{m\beta}\frac{\partial\mu}{\partial n}\Big|_{\bar{n}}\left(\frac{1}{r}+\lambda\right), \tag{C6}$$

which will be important in the following.

Second, in the limit $\int_r^\infty m\beta u$ negligible it is true that for $r>r_s$, $4\pi r^2 nu \le 4\pi r_s^2 n_- u_-$, where, again, n_- and u_- are the values of n and u at r slightly larger than r_s. Further, $4\pi r^2 nu$ stays near the upper limit as r gets large. As an approximation this will be taken as an equality until the $\int_r^\infty m\beta u$ term becomes comparable to the $\frac{1}{2}mu^2$ term. Thus using (C2) and (C1) and $n\simeq n_D$

$$n^2[\mu(n_D)-\mu(n)]\simeq\frac{mr_s^4n_-^2u_-^2}{2r^4n_D^2}+\frac{m\beta r_s^2n_-u_-}{n_D}\left(\frac{1}{r}-\frac{1}{r_s}\right). \tag{C7}$$

The two terms on the right-hand side of (C7) become comparable at an r^* defined by

$$(r_s/r^*)^4=-(6\beta\tau n_D/n_0)[(r_s/r^*)-1], \tag{C8}$$

if $n_-u_-\simeq n_0r_s/3\tau$.

Now insist that at r^* the two solutions match. This requires that (C6) be satisfied, i.e.,

$$-\frac{r_s^3n_0}{3\tau n_Dr^{*2}(n_D-\bar{n})}\simeq\frac{1}{m\beta}\frac{\partial\mu}{\partial n}\Big|_{\bar{n}}\left(\frac{1}{r^*}+\lambda\right). \tag{C9}$$

Equation (C9) is quadratic in $1/r^*$ and may be solved in standard fashion to give

$$\frac{1}{r^*}=-\frac{3\tau(n_D-\bar{n})}{2r_s^3n_0}\left\{-\frac{1}{m\beta}\frac{\partial\mu}{\partial n}\Big|_{\bar{n}}+\left[\left(\frac{1}{m\beta}\frac{\partial\mu}{\partial n}\Big|_{\bar{n}}\right)^2-\frac{4\lambda}{m\beta}\frac{\partial\mu}{\partial n}\Big|_{\bar{n}}\frac{r_s^3n_0}{3\tau n_D(n_D-\bar{n})}\right]^{1/2}\right\}, \tag{C10}$$

where the plus sign is chosen since by (C2) $n_D \lesssim \bar{n}$. Equations (C8), (C9), and (29) which yield

$$p(n_0) - p(n_D) \simeq \frac{m n_0^2 r_s^2}{n_D 36\tau^2}\left(1 - \frac{6\beta\tau n_D}{n_0}\right), \tag{C11}$$

are sufficient to determine n_0, n_D, and r_s in terms of $\bar{n}$.

From (C8) and (C11) it is clear that the key parameter is $6\beta\tau n_D/n_0$ which is $\gtrsim \eta \equiv 6\beta\tau n_g/n_l$. At low temperatures or short lifetimes $\eta \ll 1$ and it is clear that the effect of the friction term is a small perturbation. This satisfies the requirement for applicability of the hydrodynamic theory that the effect of the dissipative terms is negligible in low-density regions of the phase diagram where particle interactions are weak. At high temperatures or long lifetimes $\eta \gg 1$ and the friction term becomes extremely important.

Let us, therefore, consider solution of (C8)–(C11) in these two limits. First, when $\eta \gg 1$ one has from (C8) that $r^* \simeq r_s$. Then from (C9) and (C11), and assuming $1/r_s \gg \lambda$, one finds

$$n_D - \bar{n} = 2\frac{[p(n_D) - p(n_0)]}{n_D}\left.\frac{d\mu}{dn}\right|_{\bar{n}}, \tag{C12}$$

so that n_D, n_0 go to constants independent of β, τ, or m. One may show from (C12) that to a good approximation n_D is only slightly less than n_g and $n_0 \simeq n_l$. Then, from (C11) and (C12)

$$r_s^2 \simeq 3\tau(\bar{n} - n_g) n_g \, d\mu/dn\,|_{\bar{n}}/m n_l \beta\,, \tag{C13}$$

and the velocity at the droplet surface is

$$u_-^2 \simeq 2(\bar{n} - n_g)c^2/\bar{n}\eta\,, \tag{C14}$$

where c is the speed of sound. Hence, for $\eta \gg 1$ the velocity is always much less than the speed of sound, and r_s decreases with increasing β.

Consider next the other limit $\eta \ll 1$. Then from (C8)

$$(r_s/r^*)^4 \simeq 6\beta\tau n_D/n_0\,. \tag{C15}$$

If $1/r^* \ll \lambda$ from (C9) one obtains

$$r_s^2 \simeq \frac{3(n_D - \bar{n})^2 n_D \, d\mu/dn\,|_{\bar{n}}}{2\beta^2 n_0 \bar{n} m}, \tag{C16}$$

and

$$n_D - \bar{n} \simeq -12\tau^2 \bar{n}\beta^2\left[-1 + \left(1 + \frac{p(n_0^*) - p(\bar{n})}{8\tau^2 \bar{n} n_0^* \beta^2 d\mu/dn\,|_{\bar{n}}}\right)^{1/2}\right], \tag{C17}$$

where n_0^* is defined by $\mu(n_0^*) = \mu(\bar{n})$. From (C16) and (C17) it is clear that at sufficiently large supersaturation, $S \equiv \bar{n}/n_g - 1$, the droplet size tends to a value independent of β. At smaller supersaturation the droplet size is reduced below its size in the $\beta \to 0$ limit. For extremely small supersaturation the assumption $1/r^* \ll \lambda$ is no longer satisfied, but the appropriate result may again be obtained from (C8)–(C11).

It is evident from this analysis that $\eta \simeq 1$ defines a temperature T' separating two regimes of droplet behavior. For $\eta \ll 1$ and $T < T'$, the droplet size is limited only by a requirement that the external velocity not exceed the sound speed. For $\eta \gg 1$ and $T > T'$ the external velocity is always less than the sound speed and according to (C13) for large $\bar{n} \gg n_g$ the droplet size is only a weak function of $\bar{n}$. Evidence for a limiting droplet size has been observed by Bagaev *et al.*[2] and interpreted as being due to effects of a friction constant. There is also an alternative explanation for this behavior due to Keldysh[31] in terms of phonons emitted during recombination within droplets. Inclusion of these phonon effects would require an extension of the present model.

APPENDIX D: CELL MODEL FOR INTERACTING DROPLETS

In this Appendix it is shown how the hydrodynamic model may be applied to high excitation rates $\bar{n}/n_g \gg 1$ and how the $\lim_{r\to\infty} 4\pi r^2 n u \neq 0$ pathology of the $\beta \to 0$ limit of the hydrodynamic model is removed. The approach is to describe interacting droplets. The problem is to determine droplet size r_s, gas phase density, and droplet density n_0 as functions of the concentration of droplets N, excitation level $\bar{n}$, and temperature. It is assumed that N is determined by the history of the excitation process.[6,7]

The model proposed is that each droplet may be considered to occupy a spherical cell of volume $1/N = \frac{4}{3}\pi r_c^3$, where r_c is the cell radius. If n_c is the density at the cell surface, $n_c < \bar{n}$, and $u(r_c) = 0$, one may derive as in Sec. IV and Appendix B, that

$$p(n_0) - p(n_c) \simeq \int_0^{r_s} dr\left(\frac{1}{n_-} - \frac{1}{n_+}\right)\frac{d}{dr}\left(\frac{m n^2 u^2}{2}\right) + \frac{2K}{r_s}\int_{r_+}^{r_-}\left(\frac{dn}{dr}\right)^2 dr \tag{D1}$$

for r_s below the sound velocity limit. Here $\mu(n_0) = \mu(n_c)$. This relation determines r_s in terms of n_c.

The sole difference in the model from Sec. IV is the behavior at $r_c > r > r_s$. One has

$$0 \simeq \tfrac{1}{2} m u^2 + \mu(n) - \mu(n_c) \tag{D2}$$

and Eq. (16) determine the density profile in the $r > r_s$ region. For an approximate analysis for the relation of n_c to $\bar{n}$ and N, let n in the integrand of (16) be equal to n_0 for $r < r_s$ and n_c for $r > r_s$. Then $u(r_c) = 0$ gives

$$n_c \simeq (\bar{n} - NVn_0)/(1 - NV) . \quad \text{(D3)}$$

Here $V = \frac{4}{3}\pi r_s^3$. One must have $n_s > n_c > n_{\min}$ which restricts the range over which N and $\bar{n}$ can vary. The variation of nucleation rates with n_c may place an even more restrictive limit on the variation of N and $\bar{n}$.

It is possible that a cell model might also be used for $n_c > n_s$. In this case the density increases as one approaches the droplet surface. The constraint is that the cell size must be small enough that long-wavelength spinodal instabilities of the type described by Eq. (53) cannot occur. A stability analysis, perhaps using the Riemann method of characteristics, is required.

APPENDIX E: RELEVANT EQUATIONS OF NUCLEATION KINETICS

The droplet growth equation is[6,7]

$$\frac{dR_N}{dt} = \frac{v_{ex} n}{n_l} - \frac{v_{ex}}{n_l} n_g \exp\left(\frac{2\sigma}{R_N n_l kT}\right) - \frac{N}{\tau^4 \pi R_N^2 n_l} , \quad \text{(E1)}$$

where $v_{ex} = (kT/2\pi m)^{1/2}$ and N equals $\frac{4}{3}\pi R_N^3 n_l$. The minimum supersaturation and minimum stable radius are determined by $dR_N/dt = 0$ and $d/dN(dR_N/dt) = 0$. This gives

$$x^2 e^x = 2\sigma/3kTv_{ex} n_g \tau , \quad \text{(E2)}$$

and

$$n = n_g e^x + 2\sigma/xkT3\tau v_{ex} , \quad \text{(E3)}$$

where

$$x = 2\sigma/R_N n_l kT . \quad \text{(E4)}$$

It is interesting to put these equations into the scaled variables defined in Sec. II C. Then

$$x^2 e^x = (\tfrac{8}{9}\pi\xi)^{1/2}(1/\tilde{T}^{3/2}\tilde{n}_g) , \quad \text{(E2')}$$

$$\tilde{n} = \tilde{n}_g e^x + (\tfrac{8}{9}\pi\xi)^{1/2}(1/x\tilde{T}) , \quad \text{(E3')}$$

and

$$x = 2/\tilde{R}\tilde{T} . \quad \text{(E4')}$$

The scaled equations can be used to make predictions which can directly be compared with hydrodynamics in the region of ideal-gas behavior where nucleation kinetics is applicable. High temperatures may be defined by $\xi^{1/2}/\tilde{n}_g \ll 1$. In this limit

$$\tilde{R}_{\min} \simeq \left(\frac{18}{\pi\xi}\right)^{1/4} \frac{\tilde{n}_g^{1/2}}{\tilde{T}^{1/4}} , \quad \text{(E5)}$$

and the supersaturation is approximately

$$S_{\min} \equiv (\tilde{n} - \tilde{n}_g)/\tilde{n}_g \simeq \frac{1}{\tilde{n}_g^{1/2}} (\tfrac{8}{9}\pi\xi)^{1/4} (1/\tilde{T}^{3/4} + 1/\tilde{T}^{1/4}) . \quad \text{(E6)}$$

A temperature T_0 defined by $S_{\min} = 1$ can be determined from (E6) and is tabulated for various electron-hole liquids in Table I as discussed in Sec. II D.

At lower temperatures x becomes large and approaches $3.5/\tilde{T}$ if $\Phi_\infty/kT_c \simeq 3.5$. Thus, the minimum density for the existence of droplets approaches a temperature-independent value

$$\tilde{n}_{\min} \geq (\tfrac{8}{9}\pi\xi)^{1/2}(1/3.5) . \quad \text{(E7)}$$

These equations are to be compared to Eqs. (45) and (46) of the text. It is particularly remarkable that $S_{\min} = 1$ occurs at a temperature T_0 comparable to that predicted by hydrodynamics and that the lower limit on $\tilde{n}_{\min}$ is comparable to that of hydrodynamics.

It is also of interest to calculate the limiting droplet size from (E1). In scaled units this gives

$$\tilde{r}_s \leq \tilde{n}\tilde{T}^{1/2} 3/\tilde{n}_l \xi^{1/2} (2\pi)^{1/2} , \quad \text{(E8)}$$

which differs by a factor $(2\pi)^{1/2}$ from (48).

[1] For reviews see Ya. Pokrovsky, Phys. Status Solidi A 11, 385 (1972); C. D. Jeffries, Science 189, 955 (1975); T. M. Rice, G. A. Thomas, J. C. Hensel, and T. G. Phillips, Solid State Phys. (to be published).

[2] V. S. Bagaev, N. V. Zankovets, L. V. Keldysh, N. N. Sibel'din, and V. A. Tsvetkov, Zh. Eksp. Teor. Fiz. 70, 1501 (1976). [Sov. Phys.-JETP 43, 783 (1976)].

[3] B. Etienne, C. Benoit à la Guillaume, and M. Voos, Phys. Rev. B 14, 712 (1976); Phys. Rev. Lett. 35, 536 (1975).

[4] T. K. Lo, B. J. Feldman, and C. D. Jeffries, Phys. Rev. Lett. 31, 224 (1973); R. M. Westervelt, J. L. Staehli, and E. E. Haller, Bull. Am. Phys. Soc. 21, 224 (1976); J. L. Staehli, Phys. Status Solidi B 75, 451 (1976); R. M. Westervelt, *ibid.* 76, 31 (1976); R. M. Westervelt, J. L. Staehli, E. Haller, and C. D. Jeffries, Proceedings of the Oji Seminar on Physics of Highly Excited States in Solids, Japan, 1976 (unpublished).

[5] J. Shah, A. H. Dayem, and M. Combescot, Solid State Commun. (to be published).

[6] R. N. Silver, Phys. Rev. B 11, 1569 (1975); 12, 5689 (1975).

[7] R. M. Westervelt, Phys. Status Solidi B 74, 727 (1976); 75, 2 (1976).

[8] F. F. Abraham, *Homogeneous Nucleation Theory* (Academic, New York, 1974).

[9] For another approach, see Hoare and Pal, Adv. Phys. 28, 645 (1975).

[10] For a review, see B. Widom in *Phase Transitions and Critical Phenomena*, edited by C. Domb and M. S. Green (Academic, New York, 1972).

[11]J. W. Cahn and J. R. Hilliard, J. Chem. Phys. 28, 258 (1958); 31, 688 (1959).
[12]H. Buttner and E. Gerlach, J. Phys. C 6, L433 (1973); T. M. Rice, Phys. Rev. B 9, 1540 (1974); T. L. Reinecke and S. C. Ying, Solid State Commun. 14, 38 (1974); L. M. Sander, H. B. Shore, and L. J. Sham, Phys. Rev. Lett. 31, 533 (1973).
[13]For reviews, see article by D. R. Uhlmann and B. Chambers, in *Nucleation Phenomena* (American Chemical Society Publications, Washington, D.C. 1966), p. 17; see also article by J. E. Hilliard, in *Phase Transformations*, edited by H. J. Aaronson (American Society for Metals, Metals Park, Ohio, 1968), p. 497.
[14]J. S. Langer and L. A. Turski, Phys. Rev. A 8, 3230 (1973). This paper constitutes a hydrodynamic approach to nucleation in ordinary liquid-gas transitions.
[15]R. N. Silver, Solid State Commun. (to be published).
[16]For a complete discussion see, for example, J. O. Hirschfelder, C. F. Curtiss, and R. B. Bird, *Molecular Theory of Gases and Liquids* (Wiley, New York, 1964).
[17]See article by G. Gyarmathy, in *Two Phase Flow in Turbines and Separators: Theory, Instrumentation Engineering*, edited by C. H. Moore and M. J. Sieverding, (McGraw-Hill, New York, 1976).
[18]M. S. Epifanov, G. N. Galkin, E. A. Bobrova, V. S. Vavilov, in *Proceedings of Thirteenth International Conference on the Physics of Semiconductors, Rome, 1976*, edited by F. G. Fumi, (Tipografia Marves, Rome, 1976), p. 275.
[19]J. Fisk and B. Widom, J. Chem. Phys. 50, 3219 (1969).
[20]G. A. Thomas, T. G. Phillips, T. M. Rice, and J. C. Hensel, Phys. Rev. Lett. 31, 386 (1973); R. B. Hammond, T. C. McGill, and J. W. Mayer, Phys. Rev. B 13, 3566 (1976).
[21]M. Combescot and R. Combescot, Phys. Lett. A 56, 228 (1976).
[22]C. Benoit à la Guillaume and M. Voos, Solid State Commun. 11, 1585 (1972).
[23]J. Shah, M. Combescot, and A. H. Dayem, Phys. Rev. Lett. 38, 1497 (1977).
[24]W. Schmid, in Ref. 18, p. 898.
[25]J. Shah, R. F. Leheny, W. R. Harding, and D. R. Wight, Phys. Rev. Lett. 38, 1164 (1977).
[26]R. F. Leheny and J. Shah, Phys. Rev. Lett. 38, 511 (1977).
[27]T. L. Reinecke (unpublished)
[28]R. F. Leheny and J. Shah, Phys. Rev. Lett. 37, 871 (1976).
[29]J. Shah, R. F. Leheny, and W. Wiegmann (unpublished).
[30]O. Hildebrand, B. O. Faltermeier, and M. H. Pilkuhn, Solid State Commun. 19, 841 (1976).
[31]L. V. Keldysh, Pis'ma Zh. Eksp. Teor. Fiz. 23, 100 (1976) [JETP Lett. 23, 86 (1976)].